Performance Analysis of Frequency Domain Precoding Time-Reversal MISO OFDM Systems

Trung-Hien Nguyen, *Member, IEEE*, Shaghayegh Monfared, *Student Member, IEEE*, Jean-François Determe, Jérôme Louveaux, *Member, IEEE*, Philippe De Doncker, *Member, IEEE*, and François Horlin, *Member, IEEE*

***Abstract*— Time reversal (TR) recently emerged as an interesting communication technology capable of providing a good spatio-temporal signal focusing effect. New generations of large-bandwidth devices with reduced cost leverage the use of TR wideband communication systems. TR can easily be integrated into an orthogonal frequency-division multiplexing (OFDM) system by precoding the signal in the frequency domain. In this letter, we first extend the frequency-domain TR precoding to rate back-off factors (BOFs) different than one. We secondly derive a closed-form mean-square-error (MSE) expression of the received equalized symbols as a function of the BOFs and the number of antennas. The derived MSE formula is validated numerically with Rayleigh fading channels.**

***Index Terms*— Time reversal, rate back-off factor, OFDM.**

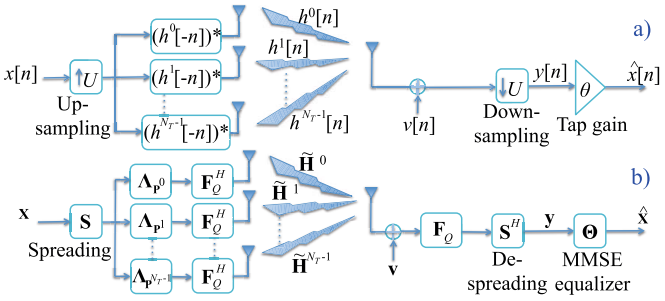

Fig. 1. Schematics of (a) the TD/TR precoding communication system [2] and (b) the corresponding FD/TR precoding OFDM system.

I. Introduction

TIME-REVERSAL (TR) with sufficient rate back-off factor (BOF) has recently gained much attention as it can combine the energy from different multipath components to create a spatio-temporal focusing effect [1]–[3]. TR precoding can be implemented in either time domain (TD) or frequency domain (FD). The TD/TR precoding has been well studied in the literature [2], [3]. The focusing effect of the TD/TR precoding comes from the use of a high BOF, which is defined as the ratio between the sampling rate and the symbol rate introduced to be capable of precoding the signal on a sufficiently large bandwidth[1] [1], [2]. Because of the spatio-temporal focusing effect of TD/TR precoding systems, a one-tap equalizer is generally sufficient in such systems, thereby lowering the receiver complexity.

Orthogonal frequency-division multiplexing (OFDM) is an efficient technology for new-generation wireless systems, thanks to its simple equalization of frequency-selective channels. The FD/TR precoding combined with OFDM has been shown to be a simple and efficient technology [4]. However, up to now, the literature [4], [5] has only considered a BOF of one, which does not exploit the full advantage of TR. Furthermore, no performance analysis of the FD/TR precoding system, i.e., mean-square-error (MSE) of the received symbols, has been provided. Recently, the performance analysis of the TD/TR system has been carried out based on the derivation of the probability density function (PDF) of signal-to-noise ratio (SNR) [3]. However, this study is limited to the single-input single-output (SISO) case and the interference analysis is omitted. In this letter, we analyze the performance of the multiple-input single-output (MISO) FD/TR system with different BOFs in order to highlight the signal-to-noise-ratio (SNR) gain given by the FD/TR precoding, similar to that provided by the TD/TR precoding. The SNR gain is defined as the reduced SNR requirement to achieve a fixed MSE when using the MISO system and/or BOFs different from 1 compared to the SISO system with BOF equal to 1. The SNR gain analysis provides us the information regarding the transmitting power that we can reduce while preserving the system MSE performance [6]. Particularly, we derive a closed-form MSE expression, and subsequently the SNR gain, for FD/TR precoding MISO OFDM systems. We validate our analysis via simulations with Rayleigh fading channels.[2]

II. System Model

The TD/TR precoding MISO system is illustrated in Fig. 1(a) [2], where the TD symbol sequence $x[n]$ is firstly up-sampled by a BOF U and repeated on N_T transmit antenna

Manuscript received September 19, 2019; revised October 18, 2019; accepted October 21, 2019. Date of publication October 25, 2019; date of current version January 8, 2020. The authors are grateful for the financial support of the Copine-IoT Innoviris project, the Icity. Brussels project and the FEDER/EFRO grant. The associate editor coordinating the review of this letter and approving it for publication was C.-K. W. Wen. *(Corresponding author: Trung-Hien Nguyen.)*

T.-H. Nguyen, S. Monfared, J.-F. Determe, P. De Doncker, and F. Horlin are with the OPERA Department, Université Libre de Bruxelles (ULB), 1050 Brussels, Belgium (e-mail: trung-hien.nguyen@ulb.ac.be).

J. Louveaux is with the ICTEAM Institute, Université Catholique de Louvain (UCL), 1348 Louvain-la-Neuve, Belgium.

Digital Object Identifier 10.1109/LCOMM.2019.2949556

[1]Alternatively, in a fixed-bandwidth system, the use of a high BOF decreases the symbol rate and therefore reduces the inter-symbol interference.

[2]*Notation*: Lower-case and upper-case bold letters denote column vectors and matrices, respectively; $\mathbf{I}_N$ is the $N \times N$ identity matrix; $\mathbf{F}_Q$ is the $Q \times Q$ Fourier matrix; $\mathbf{\Lambda}_{\mathbf{x}}$ is the diagonal matrix whose diagonal entries are the elements of the vector $\mathbf{x}$; $|\cdot|$, $||\cdot||$, $(\cdot)^*$, $(\cdot)^T$, and $(\cdot)^H$ are the absolute, Euclidean norm, complex conjugate, transpose and Hermitian transpose operators, respectively; $\mathrm{tr}\{\cdot\}$ and $\mathbb{E}[\cdot]$ are the trace and expectation operators, respectively; $x!$ is the factorial of a positive integer x.

branches. The signals are then pre-filtered by the TR precoder, $(h^k[-n])^*$, of the associated k-th channel impulse response (CIR), $h^k[n]$ before being sent over antennas. At the receiver side, the signal corrupted by additive white Gaussian noise (AWGN) $v[n]$ is down-sampled by U. It is then equalized by a tap gain θ, which can be designed based on the minimum mean square error (MMSE) criterion. It has been shown in [2] that by using more antennas and/or increasing the BOF, the spatio-temporal focusing gain improves, delivering a better bit-error-ratio (BER)/MSE performance at the cost of the symbol rate reduction. Note that, even if the received signal could directly be sampled at the low symbol rate (therefore naturally implementing the downsampling at the receiver), a wideband analog-to-digital converter (ADC) at the receiver is necessary to keep all frequency components of the received signal [6].

In the literature, the performance of FD/TR precoding OFDM system, when communicating with the target user, was only assessed for a varying number of antennas [4], while the use of different BOFs has not been studied yet. We discuss here a proper way to assign the data symbols onto OFDM subcarriers in FD/TR precoding system, as illustrated in Fig. 1(b). The number of subcarriers of one OFDM symbol is Q. For simplicity, we consider that a single OFDM symbol is sent over the TR precoding MISO OFDM system. We consider a transmit data vector $\mathbf{x} = [X_0 \ ... \ X_{N-1}]^T$ (with $N = Q/U$). The symbols $\{X_n\}$ are assumed to be independent zero-mean random variables (RVs) with variance $\mathbb{E}[|X_n|^2] = \sigma_X^2$. A normalized constellation, $\sigma_X^2 = 1$, is considered in this work.

The data symbols $\mathbf{x}$ are then spread by the matrix $\mathbf{S}$ of size $Q \times N$. The $Q \times N$ matrix $\mathbf{S}$ is the concatenation of U independent $N \times N$ diagonal matrices, whose diagonal values are identically and independently distributed and taken from the set $\{\pm 1\}$. The spreading matrix is normalized by $\sqrt{U}$ in order to get $\mathbf{S}^H\mathbf{S} = \mathbf{I}_N$. Thanks to the spreading matrix, the BOF discussed in the original TD/TR precoding is properly introduced. The idea behind this spreading comes from the fact that up-sampling a signal in the TD is equivalent to the repetition and shifting of its spectrum in the FD. Furthermore, a randomized spreading code is used to avoid assigning the same data symbol on different OFDM subcarriers, which causes a high peak-to-average-power ratio (PAPR).

After spreading, the signal is repeated on N_T branches corresponding to transmit antennas and pre-coded by a matrix $\mathbf{\Lambda}_{\mathbf{p}^k}$ on each branch k. Defining $\mathbf{h}^k := [H_0^k \ H_1^k \ ... \ H_{Q-1}^k]^T$ as the channel frequency response (CFR) associated with the $k-$th antenna and assuming its power delay profile (PDP) is normalized to unity, then $\mathbf{\Lambda}_{\mathbf{p}^k}$ is the diagonal matrix, whose diagonal elements are $(H_q^k)^*$ (for $q = 0, 1, ..., Q-1$). The FD/TR precoded signals are transformed to TD signals by using an inverse fast Fourier transform (IFFT) operator. The signal is then made cyclic by adding/removing a cyclic prefix (CP) and propagated over the channel, which is mathematically equivalent to the multiplication with the $Q \times Q$ circulant matrix $\widetilde{\mathbf{H}}^k$ of the $k-$th CIR. The matrix $\widetilde{\mathbf{H}}^k$ can be factorized as $\widetilde{\mathbf{H}}^k = \mathbf{F}_Q^H \cdot \mathbf{\Lambda}_{\mathbf{h}^k} \cdot \mathbf{F}_Q$, where $\mathbf{\Lambda}_{\mathbf{h}^k}$ is the diagonal matrix, whose diagonal elements are the elements of vector $\mathbf{h}^k$. At the receiver, the reversed operations are carried out. Note that, a wideband ADC is required and a high sampling rate is needed, as in conventional OFDM systems. However, the de-spreading operation reduces the sample rate to the symbol rate, thereby enabling the receiver to work at a *low-rate processing*. Assuming the time and frequency synchronization is perfect, the received signal after de-spreading is given by

$$\mathbf{y} = \mathbf{S}^H \cdot \mathbf{F}_Q \cdot \left(\sum_{k=0}^{N_T-1} \widetilde{\mathbf{H}}^k \cdot \mathbf{F}_Q^H \cdot \mathbf{\Lambda}_{\mathbf{p}^k} \right) \cdot \mathbf{S} \cdot \mathbf{x} + \mathbf{v}', \quad (1)$$

where $\mathbf{v}' = \mathbf{S}^H\mathbf{F}_Q\mathbf{v} := [V_0' \ ... \ V_{N-1}']^T$ is the equivalent FD circularly symmetric complex AWGN of the TD AWGN $\mathbf{v}$. We assume that the signal X_n and noise V_n' are independent of each other. We define the noise auto-correlation matrix as $\mathbf{R}_{\mathbf{vv}} := \mathbb{E}\left[\mathbf{v} \cdot \mathbf{v}^H\right] = \sigma_V^2\mathbf{I}_Q$, where σ_V^2 is the variance of $\mathbf{v}$. Based on the definition of the spreading matrix, we can deduce $\mathbf{R}_{\mathbf{v'v'}} = \sigma_V^2\mathbf{I}_N$. After some manipulations, (1) can be rewritten as $\mathbf{y} = \mathbf{G}\cdot\mathbf{x}+\mathbf{v}'$, where $\mathbf{G} = \mathbf{S}^H \cdot \left(\sum_{k=0}^{N_T-1} \mathbf{\Lambda}_{\mathbf{h}^k} \cdot \mathbf{\Lambda}_{\mathbf{p}^k}\right) \cdot \mathbf{S}$.

Similarly to the TD/TR system, we use a one-tap MMSE equalizer after de-spreading in order to recover the transmitted signal. By multiplying $\mathbf{y}$ with the MMSE equalizer matrix, given by $\mathbf{\Theta} = \left(\mathbf{G}^H \cdot \mathbf{G} + \gamma^{-1}\mathbf{I}_N\right)^{-1} \cdot \mathbf{G}^H$ (in which $\gamma := \sigma_X^2/\sigma_V^2$ is the definition of the SNR), we obtain the estimate $\widehat{\mathbf{x}}$ of the input signal vector. Note that if the TR precoding is matched to the channel, $\mathbf{\Theta}$ is a real-valued diagonal matrix, leading to a *low-complexity equalizer* at the receiver.

III. Performance Assessment and Discussion

By defining $\mathbf{e} := \mathbf{x} - \widehat{\mathbf{x}}$ and $\mathbf{R}_{\mathbf{ee}} := \mathbb{E}\left[\mathbf{e} \cdot \mathbf{e}^H\right]$, the MSE of the equalized received symbol can be derived as follows[3]

$$MSE = \mathrm{tr}\left\{\mathbf{R}_{\mathbf{ee}}\right\} = \sigma_V^2 \mathrm{tr}\left\{\mathbb{E}\left[\left(\mathbf{G}^H \cdot \mathbf{G} + \gamma^{-1}\mathbf{I}_N\right)^{-1}\right]\right\}.$$

In order to assess the SNR gain of FD/TR precoding when increasing the number of antennas and/or BOF, we define the normalized MSEs (NMSEs) as $NMSE := MSE/\left(N\sigma_X^2\right)$. The NMSE is approximated by

$$NMSE \approx \mathbb{E}\left[\frac{\gamma^{-1}}{\frac{1}{U^2}|K_n|^2 + \gamma^{-1}}\right], \quad (2)$$

where $K_n = \sum_{k=0}^{N_T-1}\sum_{u=0}^{U-1}\left|H_{n+uN}^k\right|^2$ is a RV depending on the channel realization. Note that, a Rayleigh fading channel is considered in our case. The MSE approximation is made possible due to the fact that RVs H_{n+uN}^k and $H_{n+(u+1)N}^k$ (for $\forall n \in [0, N-1]$, $\forall k \in [0, N_T-1]$ and $\forall u \in [0, U-2]$) can be considered to be independent[4] and identically distributed[5] (i.i.d.) from one another [7]. We assume that the CIRs between

[3]In what follows, the expectations are implicitly taken over the transmitted signal, noise and channel RVs.

[4]When BOF is big, H_{n+uN}^k and $H_{n+(u+1)N}^k$ are weakly correlated. The CFR correlation coefficient associated with the OFDM subcarriers p and q is $\rho_{q-p} = \mathbb{E}\left[H_p H_q^*\right] = \sum_{l=0}^{L-1}\sigma_{h_l}^2 \exp\left(j2\pi\left(q-p\right)l/Q\right)$.

[5]The CFR components, obtained by Fourier transform of the CIR of the Rayleigh fading channel with a normalized PDP become a set of identically distributed RVs.

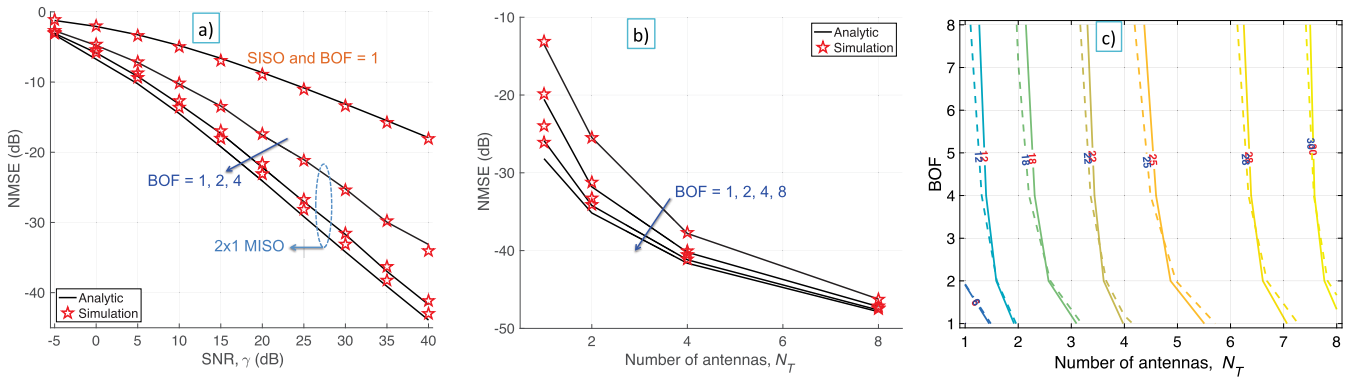

Fig. 2. a) NMSE as a function of SNR for different BOFs in the 2×1 MISO OFDM system. b) NMSE as a function of the number of antennas for different BOFs when the SNR = 30 dB. c) SNR gain contour for NMSE = -10 dB (the solid (resp. dashed) lines are the numerical (resp. analytical) results).

each transmit antenna and the receive antenna comprise no more than L taps and are independent. The CIR taps are independent (i.e., constructed by uncorrelated scatterers) and the variance of the l-th CIR tap is $\sigma_{h_l}^2 = \mathbb{E}\left[|h_l|^2\right]$.

Theorem: The closed-form NMSE approximation, $f(\gamma, U, N_T)$, of the FD/TR precoding MISO system is presented in (3), as shown at the bottom of this page, in which $\Gamma_{low}(a,t) = \int_0^t x^{a-1}\mathrm{e}^{-x}dx$ and $\Gamma_{up}(a,t) = \int_t^\infty x^{a-1}\mathrm{e}^{-x}dx$ are the lower and upper incomplete Gamma functions, respectively, such that $\Gamma_{low}(a,t) + \Gamma_{up}(a,t) = \Gamma(a)$ is the Gamma function.

Proof: The derivation is based on the first-order Taylor expansion (see the Appendix).

Corollary: The SNR gain at a certain NMSE is computed as $SNR_{gain} = SNR_{SISO} - SNR_{MISO}$ subject to $f(SNR_{MISO}, U, N_T) = f(SNR_{SISO}, 1, 1)$.

At high SNRs: We have $U\gamma^{-1/2} \approx 0$, therefore $\Gamma_{low}\left(s, U\gamma^{-1/2}\right) \approx 0$ and $\Gamma_{up}\left(s, U\gamma^{-1/2}\right) \approx \Gamma(s)$. The NMSE at high SNR, $f_{high}(\gamma, U, N_T)$, can be approximated by $f_{high}(\gamma, U, N_T) \approx U^2\gamma^{-1}\Gamma(UN_T - 2)/(UN_T - 1)!$

In the case a is a positive integer, $\Gamma(a) = (a-1)!$. Considering $UN_T > 2$, $f_{high}(\gamma, U, N_T)$ is further simplified as follows

$$f_{high}(\gamma, U, N_T) \approx \frac{\gamma^{-1}}{(N_T - 1/U)(N_T - 2/U)} \overset{U\to+\infty}{\to} \frac{\gamma^{-1}}{(N_T)^2}.$$

It reveals that when the BOF is sufficiently high, the NMSE can only be reduced by increasing the number of antennas, as shown later in the simulations.

At low SNRs: The proposed NMSE approximation $f_{low}(\gamma, U, N_T)$ is $f_{low}(\gamma, U, N_T) \approx \Gamma_{low}\left(UN_T, U\gamma^{-1/2}\right)/(UN_T - 1)!$, because in (3) the second term is smaller than the first term, whereas the third term is approximately equal to 0. Using the series expansion of the lower incomplete Gamma function $\Gamma_{low}(a,t) = t^a\Gamma(a)\mathrm{e}^{-t}\sum_{k=0}^{\infty} t^k/\Gamma(a+k+1)$ [8, eqs. (8.2.6) and (8.7.1)] and after some manipulations,

TABLE I
PDP OF THE EXTENDED PEDESTRIAN A (EPA) CHANNEL

Excess tap delay (ns)	Relative power (dB)
0	0.0
30	-1.0
70	-2.0
90	-3.0
110	-8.0
190	-17.2
410	-20.8

we can obtain the following approximation

$$f_{low}(\gamma, U, N_T) \approx 1 - \mathrm{e}^{-U\gamma^{-1/2}} \sum_{k=1}^{UN_T} \frac{\left(U\gamma^{-1/2}\right)^{UN_T - k}}{(UN_T - k)!}. \quad (4)$$

It can be seen that the same conclusion as for $f_{high}(\gamma, U, N_T)$ can be drawn from (4). If the BOF U is sufficiently high, the $f_{low}(\gamma, U, N_T)$ can only be reduced by increasing the number of antennas N_T. Because for a fixed value of N_T, the term $\mathrm{e}^{-U\gamma^{-1/2}}$ reduces faster than the summation term of (4) when increasing U, resulting in an un-changed $f_{low}(\gamma, U, N_T)$ value if U is sufficiently high. In the case U is set to a certain value, $f_{low}(\gamma, U, N_T)$ value can still be reduced further when increasing N_T as more terms are added in the summation.

IV. Simulation Results

We consider a 256-subcarrier MISO OFDM system, i.e., $Q = 256$, with a CP equal to 32. A Rayleigh fading channel of type Extended Pedestrian A (EPA) [9] is used in the simulations with its PDP given in Table I. Unless otherwise stated, numerical and analytical results are presented by the marker symbols and solid-lines, respectively.

In the first step, the NMSE is plotted as a function of the SNR in Fig. 2(a) compared to the NMSE of the SISO case with BOF of 1. The number of antennas is set to 2 and the BOFs are 1, 2 and 4. As expected, the analytical closed-form

$$f(\gamma, U, N_T) \approx \frac{1}{\Gamma(UN_T)}\left(\Gamma_{low}\left(UN_T, U\gamma^{-1/2}\right) - \frac{1}{U^2\gamma^{-1}}\Gamma_{low}\left(UN_T + 2, U\gamma^{-1/2}\right) + U^2\gamma^{-1}\Gamma_{up}\left(UN_T - 2, U\gamma^{-1/2}\right)\right) \quad (3)$$

NMSEs match the ones obtained by simulations, confirming the correctness of our derivation. The simulation results also confirm our previous observation that when increasing the BOF, the NMSE (and hence the spatio-temporal focusing) improves. For instance, in order to maintain a NMSE $=-10$ dB, with BOF $=1$, we only obtain a SNR gain of about 12 dB, while by increasing the BOF to 2 and 4, the achievable SNR gains are 16 dB and 17 dB, respectively.

In the second step, we set the SNR to 30 dB. We investigate the NMSE values when varying the number of antennas and BOFs (Fig. 2(b)). Again, the analytical results match the numerical ones. As suggested in the analysis in Section III, the NMSE does not improve further when the BOF is sufficiently high. In this case, we can improve the NMSE by increasing the number of antennas.

Finally, Fig. 2(c) illustrates the number of antennas/BOFs trade-off possible to achieve different values of the SNR gain indicated on the different lines. The SNR gain is computed to ensure the NMSE if fixed to -10 dB. The numerical results confirm again the observation made in the analyses. It should be reminded that when the BOF value is high, the assumption of the statistical independence among RVs H_n does not hold so that there are some mismatches between the analytical and numerical results.

Intuitively, the RV K_n is built constructively thanks to the TR precoding of the signal with the corresponding CFR. This leads to the reduction of the NMSE and hence improves the SNR gain, especially when increasing BOFs (associated with the frequency diversity gain). In the case we increase the number of antennas, the NMSEs are also reduced thanks to the spatial diversity gain, which confirms the results of previous works [4], [5].

V. Conclusion

We have presented a proper way to perform FD/TR precoding in MISO OFDM communication systems. By deriving the NMSE, we have shown that, similar to the TD/TR precoding, increasing either the BOF or the number of antennas improves the SNR gain of the system. The derived closed-form NMSE approximations and SNR gain have been validated through simulations, confirming the correctness of our derivations.

Appendix

The RV K_n has the PDF $f_Z(z)=z^{M-1}\mathrm{e}^{-z}/\Gamma(M)$ [10], where $M=UN_T$, (2) can then be rewritten as

$$NMSE=\int_0^{\infty}\frac{\gamma^{-1}}{z^2/U^2+\gamma^{-1}}\frac{z^{M-1}}{\Gamma(M)}\mathrm{e}^{-z}dz = \frac{\gamma^{-1}}{\Gamma(M)}\left(\int_0^{U\gamma^{-1/2}}\frac{z^{M-1}\mathrm{e}^{-z}dz}{z^2/U^2+\gamma^{-1}}+\int_{U\gamma^{-1/2}}^{\infty}\frac{z^{M-1}\mathrm{e}^{-z}dz}{z^2/U^2+\gamma^{-1}}\right) \tag{5}$$

Splitting the NMSE formula into two parts $T_1=\int_0^{U\gamma^{-1/2}}\frac{\gamma^{-1}}{z^2/U^2+\gamma^{-1}}z^{M-1}\mathrm{e}^{-z}dz$ and $T_2=\int_{U\gamma^{-1/2}}^{\infty}\frac{\gamma^{-1}}{z^2/U^2+\gamma^{-1}}z^{M-1}\mathrm{e}^{-z}dz$ ensures that the integrals can be simplified in the two ranges of interest. More particularly, T_1 can be rewritten as

$$T_1=\int_0^{U\gamma^{-1/2}}\left(1+\frac{z^2}{U^2\gamma^{-1}}\right)^{-1}z^{M-1}\mathrm{e}^{-z}dz \approx \int_0^{U\gamma^{-1/2}}\left(1-\frac{z^2}{U^2\gamma^{-1}}\right)z^{M-1}\mathrm{e}^{-z}dz, \tag{6}$$

where the approximation is achieved by using the Taylor expansion $(1+x)^{-1}=\sum_{n=0}^{\infty}(-x)^n$ that converges on the range of the integral $\left(0,U\gamma^{-1/2}\right)$, as $z^2/\left(U^2\gamma^{-1}\right)<1$. Substituting the lower incomplete Gamma function defined in Section III, we obtain the closed-form expression of T_1

$$T_1\approx\ \Gamma_{low}\left(M,U\gamma^{-1/2}\right)-\tfrac{1}{U^2\gamma^{-1}}\Gamma_{low}\left(M+2,U\gamma^{-1/2}\right).$$

Due to the fact that $U^2\gamma^{-1}/z^2<1$, we can apply again the Taylor expansion to T_2 that ensures the convergence on the range of the integral $\left(U\gamma^{-1/2},\infty\right)$, T_2 can be rewritten as

$$T_2=\int_{U\gamma^{-1/2}}^{\infty}U^2\gamma^{-1}z^{-2}\left(1+\frac{U^2\gamma^{-1}}{z^2}\right)^{-1}z^{M-1}\mathrm{e}^{-z}dz \approx \int_{U\gamma^{-1/2}}^{\infty}U^2\gamma^{-1}z^{M-3}\mathrm{e}^{-z}dz = U^2\gamma^{-1}\Gamma_{up}\left(M-2,U\gamma^{-1/2}\right). \tag{7}$$

Finally, substituting the derived T_1 and T_2 into (5) and using the fact that $M=UN_T$, we achieve the closed-form NMSE approximation as in (3).

References

[1] Y. Chen, Y.-H. Yang, F. Han, and K. J. R. Liu, "Time-reversal wideband communications," *IEEE Signal Process. Lett.*, vol. 20, no. 12, pp. 1219–1222, Dec. 2013.

[2] M. Emami, M. Vu, J. Hansen, A. J. Paulraj, and G. Papanicolaou, "Matched filtering with rate back-off for low complexity communications in very large delay spread channels," in *Proc. Conf. Rec. 38th Asilomar Conf. Signals, Syst. Comput.*, vol. 1, Nov. 2004, pp. 218–222.

[3] W. Lei and L. Yao, "Performance analysis of time reversal communication systems," *IEEE Commun. Lett.*, vol. 23, no. 4, pp. 680–683, Apr. 2019.

[4] T. Dubois, M. Hélard, M. Crussière, and C. Germond, "Performance of time reversal precoding technique for MISO-OFDM systems," *EURASIP J. Wireless Commun. Netw.*, vol. 2013, no. 1, p. 260, 2013.

[5] T.-H. Nguyen, M. Van Eeckhaute, J.-F. Determe, J. Louveaux, P. De Doncker, and F. Horlin, "Analysis of residual CFO impact on downlink massive MISO systems," *Electron. Lett.*, vol. 55, no. 18, pp. 1017–1019, Sep. 2019.

[6] Y. Chen, B. Wang, Y. Han, H.-Q. Lai, Z. Safar, and K. J. R. Liu, "Why time reversal for future 5G wireless? [Perspectives]," *IEEE Signal Process. Mag.*, vol. 32, no. 2, pp. 17–26, Mar. 2016.

[7] T.-H. Nguyen, J.-F. Determe, M. Van Eeckhaute, J. Louveaux, P. De Doncker, and F. Horlin, "Frequency-domain time-reversal precoding in wideband MISO OFDM communication systems," Apr. 2019, *arXiv:1904.10727*. [Online]. Available: https://arxiv.org/abs/1904.10727

[8] *NIST Digital Library of Mathematical Functions*. Accessed: May 10, 2019. [Online]. Available: https://dlmf.nist.gov/8

[9] *User Equipment (UE) Radio Transmission and Reception; 3rd Generation Partnership Project; Technical Specification Group Radio Access Network; Evolved Universal Terrestrial Radio Access (E-UTRA)*, document 3GPP TS 36.101. [Online]. Available: http://www.3gpp.org

[10] A. Papoulis, *Probability—Random Variables and Stochastic Processes*, 3rd ed. New York, NY, USA: McGraw-Hill, 1991.